Volume 25
Number 7
7 April 2023
Pages 2469-2882

Green Chemistry

Cutting-edge research for a greener sustainable future

rsc.li/greenchem

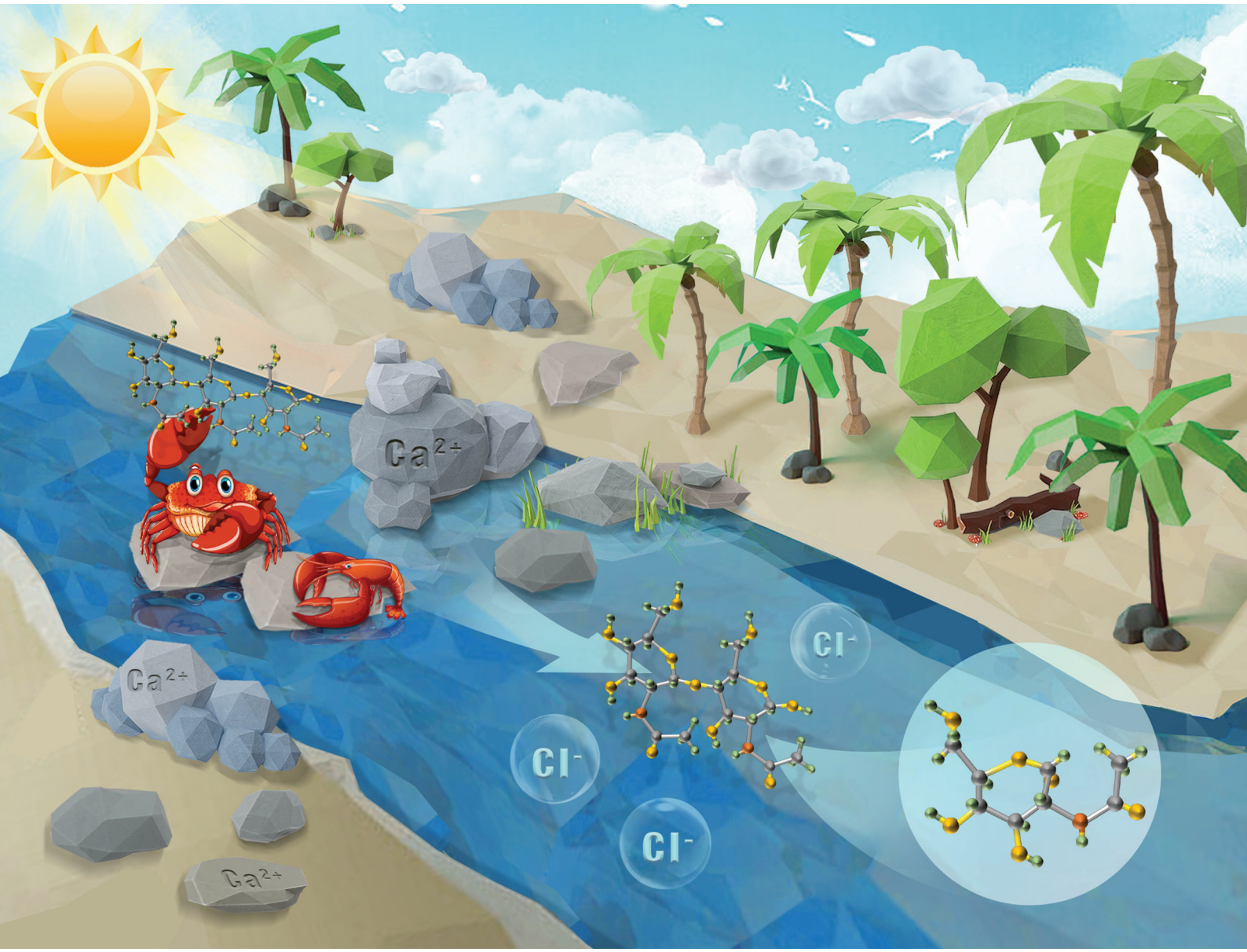

ISSN 1463-9262

ROYAL SOCIETY OF CHEMISTRY

PAPER
Xi Chen *et al.*
Acid hydrolysis of chitin in calcium chloride solutions

Green Chemistry

PAPER

View Article Online
View Journal | View Issue

Cite this: *Green Chem.*, 2023, **25**, 2596

Acid hydrolysis of chitin in calcium chloride solutions†

Yudi Wang, Jia Kou, Xuewei Wang and Xi Chen *

Received 11th November 2022,
Accepted 29th January 2023

DOI: 10.1039/d2gc04246k

rsc.li/greenchem

Chitin hydrolysis is an important but challenging reaction for shell biorefineries. In this study, we devised a mild aging-hydrolysis integrated approach to selectively produce *N*-acetyl-D-glucosamine (NAG) from chitin in cheap and abundant $CaCl_2$-based molten salt hydrate solvents (MSHs). The acid-aged chitin could be directly employed and hydrolyzed in 50 wt% $CaCl_2$ solution at 393 K for 1 h, producing NAG in 51.0% yield, which was further improved to 66.8% with the addition of $ZnBr_2$ (10 wt%) as a co-salt. The synergy of aging and the $CaCl_2$ MSHs was critical for the efficient chitin hydrolysis. A significant decrease of chitin's molecular weight was observed after aging at near room temperature, while the $CaCl_2$ MSHs enabled chitin swelling and dissolution to facilitate the substantial cleavage of glycosidic bonds during the hydrolysis reaction. The combined contrast experiments, TOF-MS, XPS, and NMR studies revealed that both the Ca^{2+} cation and the Cl^- anion have closely interacted with the chitin chains primarily by coordinating with the carbonyl oxygen/amido nitrogen atoms or by forming hydrogen bonds with the –OH groups, respectively, which could alter the electrostatic states of the chitin chains and favor the hydrolysis.

Introduction

Global warming has become a central environmental problem of the century due to the overwhelming consumption of non-renewable fossil fuels.[1–14] Intensive efforts have been made worldwide to fight against it through various strategies. Biomass resources are renewable, abundant, widely available and inexpensive, serving as favorable alternatives to fossil feedstocks for energy and chemical production to mitigate carbon emission.[15–28] Commercially available from shell waste, chitin is the world's second most abundant biomass (100 billion tons per year) with a linear and relatively homogeneous polymer structure mainly consisting of *N*-acetyl glucosamine (NAG) monomers linked by β-(1,4)-glycosidic bonds.[29–34] Chitin shares a similar structure to cellulose, but naturally bears the nitrogen element (as in the acetamido side chain), which offers a special platform resource to produce both organooxygen and organonitrogen chemicals.[30,35–41] Since the conception of chitin/shell biorefineries,[42] a diversity of products including sugars,[43,44] organic acids,[45–48] amino acids,[12,49] furanic derivatives,[50–55] N-heterocycles,[56,57] *etc.* have been obtained in recent years from chitin biomass or directly from waste shrimp shells by different strategies, which has expanded the boundary of biorefineries and enlarged the bio-based chemical pool.[19,58–64]

The primary step for chitin valorization is to hydrolyze it into the NAG monomer. The NAG monomer is not only a valuable product with important applications in various areas such as medical, food, cosmetic, *etc.*, but also a beneficial entry point in chitin biorefineries to access a diversity of other useful compounds.[45,58,65] Since natural chitin polymers usually have a high molecular weight (MW), high crystallinity and extensive intra- and inter-hydrogen bonds among the chains, the hydrolysis and other transformations are challenging.[66] Very concentrated mineral acid solutions (*e.g.* 12 M HCl or 15 M H_2SO_4) are often used to industrially produce NAG from chitin, which suffers from major issues such as high capital/waste treatment costs, heavy environmental burdens, low product selectivity, *etc.* This impels constant research efforts to develop new protocols for chitin hydrolysis. The biological (enzymatic) hydrolysis of chitin can be relatively mild and selective, but the slow reaction rates, expensive reagents and strict cultivation requirements are the general concerns. For the chemical hydrolysis of chitin, some treatment techniques are commonly exploited to improve the efficiency and/or diminish the environmental impacts.[67,68] For example, microwave irradiation and ultrasonication were utilized to aid chitin hydrolysis with shortened periods of time, although considerable amounts of concentrated acid solutions were also used and deacetylation seriously occurred as a side reaction.[69] The mechanochemical technology by ball milling chitin with a strong mineral acid or solid acid (for 4–6 h)

China-UK Low Carbon College, Shanghai Jiao Tong University, 3 Yinlian Rd, 201306 Shanghai, China. E-mail: chenxi-lcc@sjtu.edu.cn

†Electronic supplementary information (ESI) available. See DOI: https://doi.org/10.1039/d2gc04246k

could completely/partially transform chitin into water-soluble oligomers without evident deacetylation, which were then employed for the subsequent hydrolysis to produce NAG (53% yield at 443–463 K).[70,71] Unfortunately, such treatment techniques often require substantial energy inputs and are not convenient for scaling-up.

The solvent effect can be pronounced for chitin hydrolysis. Organic solvents such as formic acid and ethylene glycol have been used to depolymerize chitin at 373–448 K with several sugar derivatives as the main products but with relatively low product selectivity.[72,73] Meanwhile, the co-solvent system of water/diethylene glycol diethyl ether (DGDE) (1 : 4, v/v) could convert ball milled chitin into glucosamine in 80% yield with 100 mM H_2SO_4 at 448 K.[74] Despite the high yield, the less conventional solvent was neither cheap nor environmentally friendly and only deacylated sugars could be obtained. Inorganic molten salt hydrate solvents (MSHs) have been extensively used as green and efficient solvent systems for biomass depolymerization and dehydration. MSHs refer to a group of inorganic salt aqueous solutions with the water-to-salt ratio close to the coordination number of the strongest hydrated cations. The cations and anions of MSHs were reported to interact with the hydroxyl groups of biomass materials such as cellulose and promote their dissolution. Besides, the polarization of water molecules in MSHs favoured the generation of protons for biomass hydrolysis. Compared to cellulose, the application of MSHs to chitin conversion has been much less studied.[75–82] Yan's group recently disclosed an exclusive effect of acidified LiBr (60 wt%) MSHs over other salt species to hydrolyze chitin into NAG with an outstanding yield of 71.5%, which showed the great potential of MSHs for chitin hydrolysis.[83] However, concentrated Li-based solvents may not be economical and viable since Li availability has declined to an unbelievably low level with escalating prices due to the market expansion of Li-based industries. Furthermore, it is still highly attractive to explore the unresolved chemistry of an abundant, more available and inexpensive green solvent system for efficient chitin hydrolysis.[84–86]

Inspired by these works, we surmise the possibilities of coupling a mild aging step with hydrolysis in low-cost, widely available MSHs to produce NAG from chitin. $CaCl_2$ was identified as the most powerful salt species after solvent screening. Calcium is the 5th most abundant metal element in the Earth's crust and can also be extracted from seafood waste such as the shells of crabs, oysters, *etc.* $CaCl_2$ MSHs could not only swell and partially dissolve chitin but also stimulate its depolymerization. With acid aging (30 mM H_2SO_4 as in the hydrolysis step), chitin could be hydrolyzed into NAG with 51.0% yield in 50 wt% $CaCl_2$ solution, and a higher yield of 66.8% was realized by adding 10 wt% $ZnBr_2$ as a co-salt. The roles of aging and the $CaCl_2$ solvent were studied by control experiments and various characterization studies. The acid aging and $CaCl_2$-based solvents were well-cooperated to enable effective chitin hydrolysis to produce NAG. The acid dispersed on chitin induced steady depolymerization of chitin to lower MWs during aging, while the Ca^{2+} cation and Cl^- anion intensely interacted with the chitin chains during the hydrolysis to promote further scissions of the glycosidic bonds for selective NAG formation.

Results and discussion

Initial studies on the aging-hydrolysis protocol

Several ample, inexpensive and widely available MSHs including NaCl, $MgCl_2$, $CaCl_2$, $ZnCl_2$, $FeCl_2$ and $FeCl_3$ were initially attempted to hydrolyse chitin into NAG without aging. Nonetheless, NAG was not observed in most of the solvents excluding 50 wt% $CaCl_2$ solution with 4.5% yield at 393 K for 1 h (see Fig. 1). Next, an easy and mild aging step was conceived to assist the hydrolysis. A small amount of H_2SO_4 (the chitin to acid molar ratio (C/A ratio) was 8 : 1) was uniformly distributed onto chitin powders by natural evaporation of the diethyl ether solvent, and the chitin–H_2SO_4 mixture was aged in an ambient environment for 24 h. Previous literatures have reported acid impregnation (4.4–72 wt% H_2SO_4 solution at 298–513 K) of biomass for pretreatments, paste formation or other purposes.[87–90] In the mechanochemical conversions, solvent evaporation was adopted to disperse H_2SO_4 on biomass resources to prepare homogeneous samples for immediate use.[70,91–93] However, acid aging of biomass in the solid state has not yet been attempted and the aging effects remain unexplored. The aged mixture can be directly employed for hydrolysis. With aging, NAG became detectable with 1–3% yields in concentrated NaCl, $FeCl_2$ and $FeCl_3$ solutions, and encouragingly, a 3-time enhancement of NAG yield to 16.5% was realized in 50 wt% $CaCl_2$ solution under identical reaction conditions. The results show the beneficial contribution of aging and the distinct role of $CaCl_2$ MSHs on chitin hydrolysis. Despite the aging process being mild, some key structural

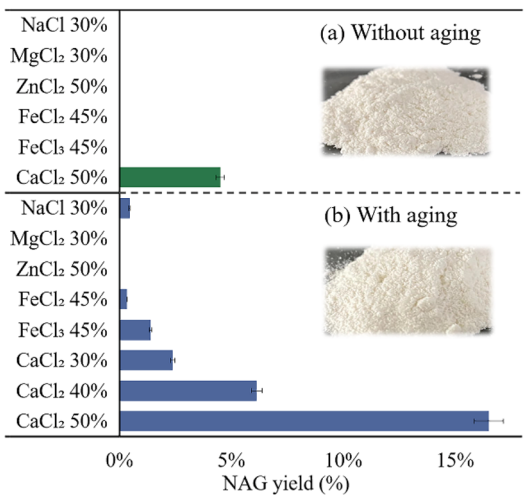

Fig. 1 Hydrolysis of (a) chitin without aging and (b) chitin with aging (aging 48 h at RT) in different types of salt solutions. Reaction conditions: 0.2 g of chitin was added in 4 mL of salt solution and heated at 393 K for 1 h. The C/A ratio was 8 : 1.

changes of chitin might occur to enable the subsequent attacks of $CaCl_2$ to promote NAG formation. The initial tests substantiate the potential of the aging-hydrolysis approach using $CaCl_2$ MSHs for chitin hydrolysis.

After aging, a minute color change from pure white to yellowish white of the powders was observed (see Fig. 1, images in the inset). The images of the chitin samples with and without aging in different solvent systems including water, NaCl (30 wt%) and $CaCl_2$ (50 wt%) are shown in Fig. S1,† and the states of chitin dissolution were compared. After stirring, the original and aged chitin in water and NaCl solutions were observed as opaque suspensions. In contrast, those in $CaCl_2$ solution looked clearer and more transparent, which were the signs for chitin swelling and dissolution. After standing still for a while, it became more obvious that considerable amounts of insoluble solids precipitated on the bottom of the tubes for the chitin samples in water and NaCl solutions, while those in $CaCl_2$ solution stayed in a similar way to colloids. This substantiates the capacity of concentrated $CaCl_2$ solution to swell and dissolve chitin polymers. With a stronger dissolution ability, chitin polymers could be more easily accessible and transformed in the concentrated $CaCl_2$ solution than water and other attempted MSHs. In addition, varied $CaCl_2$ concentrations of 30–50 wt% were tested for chitin hydrolysis, and a positive correlation between the $CaCl_2$ concentration and the NAG yield was identified. At 50 wt% salt content, the Ca^{2+} to H_2O ratio was around 1 : 6, which approximates to the maximum cation coordination number. In this regard, H_2O would tightly bind to the inner coordination sphere of Ca^{2+}, which might enhance the proton activity coefficient due to the deshielding effect and free the Cl^- anions to be more accessible to interact with the chitin chains.[94–96] Therefore, 50 wt% concentration of $CaCl_2$ MSHs is favourable.

Influences of the aging parameters

The parameters for aging were adjusted and evaluated. First, different C/A ratios (10 : 1, 8 : 1, 6 : 1 and 4 : 1) with a range of aging time periods from 24 h to 72 h were investigated. Generally, the NAG yield grew with the increase in the C/A ratio from 10 : 1 to 8 : 1/6 : 1 and then decreased at the ratio of 4 : 1 (see Fig. 2a). It suggests that the ratio of 10 : 1 was too low for efficient aging, while 4 : 1 was too high. An overdose of acid might cause undesirable side reactions when heating at 393 K for hydrolysis. When the acid ratio increased from 8 : 1 to 4 : 1 to convert chitin, the yields of by-products such as levulinic acid and lactic acid gradually increased (see Table S1,† entries 2 and 3). Additionally, the color of the reaction solution became darker (see Fig. S2†) with higher acid dosage, which possibly implies that more humins were formed as by-products. Meanwhile, the two parameters of the C/A ratio and aging time were correlated. At lower ratios (10 : 1 and 8 : 1), a constant increase of the NAG yield was noticed with the increase in aging time. In contrast, the NAG yield slightly decreased with prolonged aging time at higher ratios (6 : 1 and 4 : 1). As a result, higher acid dosage and longer aging time would not necessarily lead to better aging efficiency. Overall,

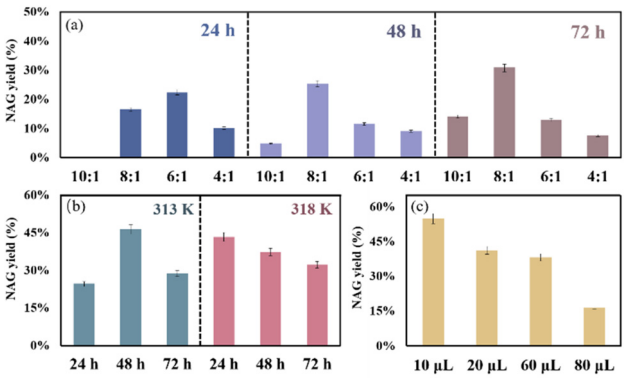

Fig. 2 The NAG yield under different chitin aging conditions. (a) At RT, the C/A ratio was 10 : 1, 8 : 1, 6 : 1 and 4 : 1 and the aging time was at a range from 24 h to 72 h; (b) at 313 K and 318 K, the C/A ratio was 8 : 1 and the aging time was at a range from 24 h to 72 h; and (c) at 313 K, the C/A ratio was 8 : 1, and the aging time was 48 h and the volume of water addition was 10 μL, 20 μL, 60 μL and 80 μL. Other reaction conditions: 0.2 g of chitin was added into 4 mL of solvent and heated at 393 K for 1 h.

the C/A ratio of 8 : 1 was observed to be optimal, obtaining a satisfactory NAG yield of 30.7% after an aging period of 72 h. Next, the aging temperature was elevated a bit to 313 K, 318 K and 328 K (see Fig. 2b). The product yield is sensitive to the aging temperature. 46.3% and 43.3% NAG yields were achieved, respectively, upon aging at 313 K for 48 h and at 318 K for 24 h. At higher aging temperatures, longer aging periods caused the NAG yield to decline, which also suggested that harsher aging conditions could probably induce NAG decomposition and decrease the yields. Besides, when aging at 328 K for 48 h, the NAG yield apparently declined to 32.3%. The HPLC analysis suggested that more by-products were generated upon using aged chitin at 328 K compared to that at 318 K (see Table S1,† entries 4 and 5), inferring more severe side reactions when aging at high temperatures.

Lastly, the influence of water on the aging performance was examined (see Fig. 2c). Small amounts of water (0.067 to 0.53 molar equivalent to chitin) were supplemented in the aging process. With 10 μL water addition (0.067 equivalent to chitin), the NAG yield slightly enhanced from 46.3% to 51.0%. However, a gradual decrease in the NAG yield was observed with a further increase in the water amount (<20% when 0.53 equivalent of water was added). The results suggest that a tiny amount of water is desirable, whereas excess amount of water is detrimental. Presumably, extra water would weaken the chemical forces of H_2SO_4 attached on chitin chains and thus impede the aging effect.[97–99]

Optimization of the reaction systems

After determining the aging parameters, the hydrolysis reaction systems were systematically optimized. First, the chitin concentration was varied from 0.025 g mL^{-1} to 0.100 g mL^{-1} (see Fig. S3†). The NAG yield was peaked with 0.050 g mL^{-1} substrate concentration, and gradually decreased with a more

concentrated chitin feedstock. The acid catalyst seemed overdosed for the diluted feedstock solutions and insufficient for the concentrated ones. Next, the influences of reaction time and temperature were studied for chitin hydrolysis. The reaction temperature was varied from 353 K to 403 K with the reaction time ranging from 15 min to 180 min (see Fig. 3). These two parameters were associated with each other and played significant roles in terms of the NAG yield. At a low temperature of 353 K, hydrolysis proceeded slowly, and no NAG was formed within the first 45 min. 11.0% NAG yield was obtained at 60 min, which then gradually increased with time to 25.0% at 180 min. The reaction rate was faster at 373 K, and a constant growth of the NAG yield was noticed, reaching 35.3% at 180 min. At 393 K, the reaction kinetics was apparently accelerated, and a volcano-shaped curve was generated with a peak value of 51.0% at 60 min. Further increasing the temperature to 403 K led to a rather rapid reaction profile with the highest NAG yield of 47.3% obtained at only 30 min. Then, a continuous decrease in the NAG yield was observed with the increase in the reaction time to merely 6.5% at 180 min. Hence, a suitable temperature of >393 K was necessary to prompt the chitin hydrolysis with a short time period and relatively higher product yield.

In addition, we have investigated the by-products of the optimal hydrolysis process. The conversion rate of chitin was determined as 73.4%, while the NAG yield was 51.0% at 393 K. Several minor by-products were observed in HPLC and quantified by using external calibration curves with authentic samples, including 5-hydroxymethylfurfural (5-HMF, 0.6%), formic acid (0.1%), levulinic acid (1.1%), 3-acetamido-5-acetylfuran (3A5AF, 0.3%), acetic acid (0.4%) and lactic acid (2.8%) (see Table S1,† entry 1). Such by-products could be derived from side reactions such as deacetylation, deamidation, dehydration, *etc*. Meanwhile, the colour of the solution changed from pale yellow to brownish black after the reaction, which probably indicates the formation of humins. We have also examined the by-products when reacting the aged-chitin at 403 K. Side products including 5-HMF, formic acid, levulinic acid, acetic acid, lactic acid and 3A5AF were identified, and some of them showed increased yields at elevated temperatures (Table S1,† entry 6). This implies more severe side reactions at 403 K compared to 393 K. Besides, starting from NAG, most of the side products were observed at the reaction temperatures of 393 K and 403 K and their yields were similar. However, the conversion rates of NAG were 51.6% and 55.7% at 393 K and 403 K, respectively, and the product of 403 K had a darker colour, which means that more humin was produced, indicating that NAG decomposition happened more severely at higher temperature (Table S1,† entries 7 and 8). Overall, the occurrence of side reactions as well as NAG decomposition could be the reasons for the decreased NAG yield. In addition, decomposition tests were conducted for NAG in water and 50 wt% $CaCl_2$ solution (see Fig. S4†). Negligible decomposition of NAG was observed in water at 393 K for 30 min and 60 min. Conversely, the decomposition rates were 32.8% and 49.8% in concentrated $CaCl_2$ solution at 393 K for 30 min and 60 min. As a result, the $CaCl_2$ solution concomitantly stimulated chitin dissolution, hydrolysis and NAG decomposition, deacetylation reaction, deamination, dehydration and other reactions, and the identification of optimal reaction conditions was essential to achieve a high product yield.

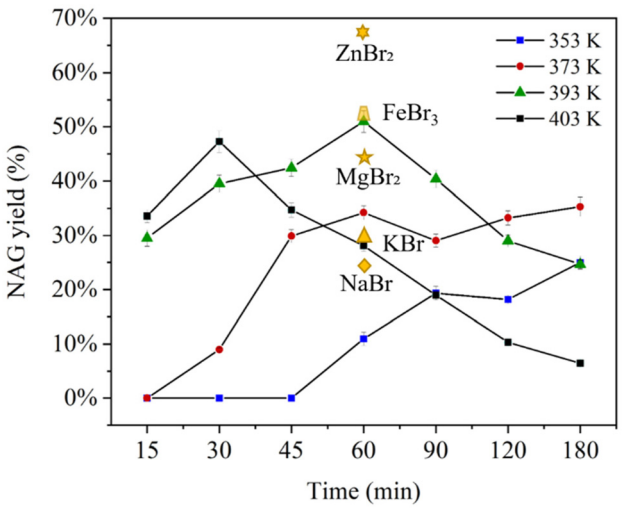

Fig. 3 The NAG yield under different reaction temperatures (353–393 K) and times (15–180 min). Chitin was aged under the optimal conditions.

To further improve the NAG yield, the combinatorial use of $CaCl_2$ and a co-salt species was considered. Five different types of bromide co-salts (10%) were attempted including NaBr, KBr, $MgBr_2$, $FeBr_3$, and $ZnBr_2$ (see Fig. 3). The addition of NaBr and KBr considerably decreased the product yield to 26.7% and 29.6%, respectively. $MgBr_2$ as a co-salt also slightly decreased the NAG yield to 44.7%, while $FeBr_3$ had little effect on the hydrolysis reaction, generating NAG in 51.2% yield. Notably, $ZnBr_2$ as a co-salt obviously increased the NAG yield to 66.8%, despite $ZnCl_2$ alone being proven as inactive for chitin hydrolysis in the initial studies. $ZnBr_2$ functions as a useful co-salt with $CaCl_2$ to facilitate chitin hydrolysis. Such improved effects of mixed salt solutions were previously reported, while the mechanism behind was still unclarified.[100] The enhancement of ionic strength and the collaborative effects might be the possible reasons. For the hydrolysis of aged chitin, the apparent activation energy (E_a) of NAG production in 50 wt% $CaCl_2$ solution was studied and estimated to be 98.9 kJ mol^{-1} by the Arrhenius plot (see Fig. S5 and Table S2†), which was a bit lower than the values of chitin hydrolysis in concentrated mineral acid and LiBr solutions (123–138 kJ mol^{-1}).[83] From the above, the integration of aging and $CaCl_2$ MSHs provide a mild, cheap but effective approach to advance the chitin hydrolysis to produce NAG in 51.0% yield (66.8% yield with 10 wt% $ZnBr_2$ co-salt), which is much higher than those obtained by traditional methods using concentrated acids.[69]

Several potential methods could be applied to purify the NAG product from the MSH system, including zeolite or amor-

phous carbon adsorption, membrane separation, ion exchange chromatography, and anti-solvent precipitation. Several studies have shown that amorphous carbon can adsorb similar products such as cellobiose and glucose from MSH.[95] In addition, membrane separation is also widely used in the separation of sugar.[101] The anti-solvent method can separate oligosaccharides.[102]

Aging effect on the chitin structure

The hydrolysis of chitin in concentrated $CaCl_2$ solution was remarkably fostered with aging. A variety of techniques have been utilized to analyze the aging-induced structural changes of chitin to illustrate the underlying mechanism (see Fig. S6†). First, the aged chitin sample was washed with water to remove the acid and subjected to Fourier transform infrared spectroscopy analysis (FTIR). In comparison with the original chitin, the FTIR spectrum of the aged chitin displayed similar characteristic peaks. This indicates that the chitin skeletons as well as the functional groups were largely preserved after aging without deacetylation. Likewise, the multifunctional X-ray diffraction (XRD) signals of the original and aged chitin samples were relatively similar. The CI values of the two aged chitin samples (chitin-RT-48 and chitin-313-48) were calculated to be 94.0% and 89.3%, respectively, which were similar to and lower than that (94.5%) of the original chitin. Hence, the increase in aging temperature might favor the destruction of the crystal domains of chitin. The influence of aging at 313 K for 48 h on the CI value was comparable to that when using 68 wt% H_3PO_4 solution to pretreat chitin polymers at 333 K for 1 h (CI decreased from 91% to 82%), despite the aging process being much milder without wastewater generation.[103] From the Scanning Electron Microscopy (SEM) images, it was seen that the surface of the aged chitin sample seemed to be rougher than that of the original chitin, which agrees with the Brunauer–Emmett–Teller (BET) analysis that the specific surface area of aged chitin increased from that ($2.2\ m^2\ g^{-1}$) of original chitin to $19.9\ m^2\ g^{-1}$.

The alterations of the crystal structure and surface area in aging seemed too inconsequential to drive such a significant enhancement in chitin hydrolysis. We then performed thermogravimetric analysis (TGA), derivative thermogravimetry (DTG) and differential scanning calorimetry (DSC) analysis (as shown in Fig. S7†). From TGA, the first stage of weight loss of chitin at around 321–376 K was ascribed to the water loss. Such a peak was insignificant for the aged chitin because the aged sample was dried before the analysis. The considerable decreases of weight in the second stage at 550 K onset was ascribed to the decomposition of chitin. The aged chitin apparently showed a lower decomposition temperature, which was consistent with the DTG results. The DSC curve, which showed both an absorption and an exothermic peak for chitin, and only an exothermic peak for aged chitin, was also consistent with the results of the TGA and DTG analyses. The aged sample showed a smaller exothermic peak area, indicating that decomposition was easier for the aged sample. Based on the results, the aged chitin has a less stable structure and may be easier to be hydrolyzed.

We noticed that chitin after aging became partially soluble in water, which might imply a dramatic change in the MWs. The solubility of various aged chitin samples were determined, and are shown in Table S3.† A gradual increase of solubility from 14.9% to 22.8% was observed when aging at RT with the acid dose increased from 10 : 1 to 4 : 1. Aging at higher temperatures of 313 K and 318 K did not lead to an obvious increase of solubility. The water-soluble fraction of chitin-313-48 was further studied by TOF-MS (see Fig. S8 and Table S4†). Groups of peaks assigned to the monomers and chito-oligomers were identified by Time-of-Flight Mass Spectrometry (TOF-MS). For instance, the main signal at m/z 204 represented the positively charged dehydrated NAG ($(C_8H_{13}NO_5)\ H^+$). The peaks centered at m/z 407, 610, 813, *etc.* were ascribed to the NAG oligomers (from dimer to pentamer). A cluster of peaks with a lower intensity at m/z 162, 365, 568 and 771 were attributed to the deacetylated oligomers, which implies that deacetylation happened to some extent for the soluble fraction.

Aside from the soluble fractions, the MWs of the original chitin and the insoluble parts of chitin-RT-48, chitin-313-48, chitin-318-48 and chitin-328-48 were evaluated by the viscometry method (see Table 1). The original chitin sample had a very large MW of around 411.3 kDa, whereas the MWs of the insoluble fractions strikingly decreased to 74.4 kDa and 42.5 kDa (about 1/5th and 1/10th of the original value) for chitin-RT-24 and chitin-313-48, respectively. The MWs were even lower (29.0 kDa and 23.2 kDa) for chitin-318-48 and chitin-328-48. Overall, the sharp decline in MWs after aging was probably responsible for the promotional effect on chitin hydrolysis. However, despite chitin-328-48 having the lowest MW, the NAG yield was not high (32.3%), possibly because of more severe side reactions (see Table S1,† entry 5). Hence, there is a balance point between aging temperature and time to obtain the most suitable aged chitin for NAG production. We conjectured that the uniformly dispersed H_2SO_4 would intimately

Table 1 The MWs of different chitin samples

Samples	η (dL g^{-1})	M_η (Da)
Chitin	16.38	411 349
Chitin-RT-48	3.23	74 430
Chitin-313-48	1.9	42 537
Chitin-318-48	1.31	29 012
Chitin-328-48	1.07	23 223
$CaCl_2$-15 min	1.94	43 634
$CaCl_2$-30 min	1.17	25 500
$CaCl_2$-60 min	0.55	11 622
Water-60 min	1.89	42 306
$CaCl_2$-10 min (no acid)	3.11	73 584
$CaCl_2$-15 min (no acid)	2.54	57 715
$CaCl_2$-20 min (no acid)	1.75	39 037

For the sample names, $CaCl_2$ or water denotes the solvent used. *XX* min indicates the reaction time; the samples were collected after a certain reaction time period by centrifugation, washing and drying. Reaction conditions: 0.2 g of the substrate in 4 mL of solvent was heated at 393 K for 1 h.

anchor onto chitin chains and serve as the active sites to kindle the cleavage of glycosidic bonds during aging. EA analysis probed the sulfur residues (about 0.4 wt%) on thoroughly washed aged chitin (washed with DI water more than three times). This implies a strong chemical adherence of H_2SO_4 on chitin (see Table S5†), which may explain the drastically decreased MWs in the mild aging environment. Besides, it could probably explain why adding a small amount of water is advantageous for aging, since water is a necessary reagent involved in the depolymerization reaction.

The functions of $CaCl_2$ in chitin hydrolysis

Our initial tests have shown that $CaCl_2$ MSHs are superior to other salt solutions for chitin swelling and dissolution. The functions of $CaCl_2$ during the hydrolysis reaction were further studied. First, the solid residues after the reactions at 393 K for 15 min, 30 min and 60 min were collected and characterized by FTIR and XRD and the viscometry method (see Fig. S9† and Table 1). From the FTIR and XRD spectra, it could be seen that the solid residues were primarily unconverted chitin polymers with identical characteristic peaks, and negligible deacetylation was observed. Only minor peak broadening and smoothing were noticed at around 3200–3500 cm^{-1}, which were related to the inter- and intra-hydrogen bonds of the –OH and –NH groups, possibly implying a slight impairment of the hydrogen bond networks of chitin. Overall, the $CaCl_2$ MSHs did not cause noticeable alternations in the functionalities and crystal structures of chitin during the reaction. In contrast, significant changes of MWs were observed. The MWs decreased considerably from 42.5 kDa to 25.5 kDa and 11.6 kDa after the reaction time periods of 30 min and 60 min. When pure water was used as the solvent in the presence of 30 mM H_2SO_4, a negligible decease in MW was found (kept at 42.3 kDa after a reaction time period of 60 min). Control experiments using the original chitin as the substrate in 50 wt% $CaCl_2$ without acid addition were conducted. A constant decrease in MWs was observed with prolonged reaction times (from 411.3 kDa to 73.6 kDa, 57.7 kDa and 39.0 kDa after reaction for 10 min, 15 min and 20 min). This further verifies the role of $CaCl_2$ in chitin depolymerization. According to the literature studies, the charged metal cations in MSHs strongly interacted with the surrounding lone pairs of the O atoms, while the H atoms turned more positively charged in the water molecules. In this way, the O–H bond was impaired to generate protons in the MSHs. Vlachos's group has recently utilized OLI thermodynamic software to match up medium

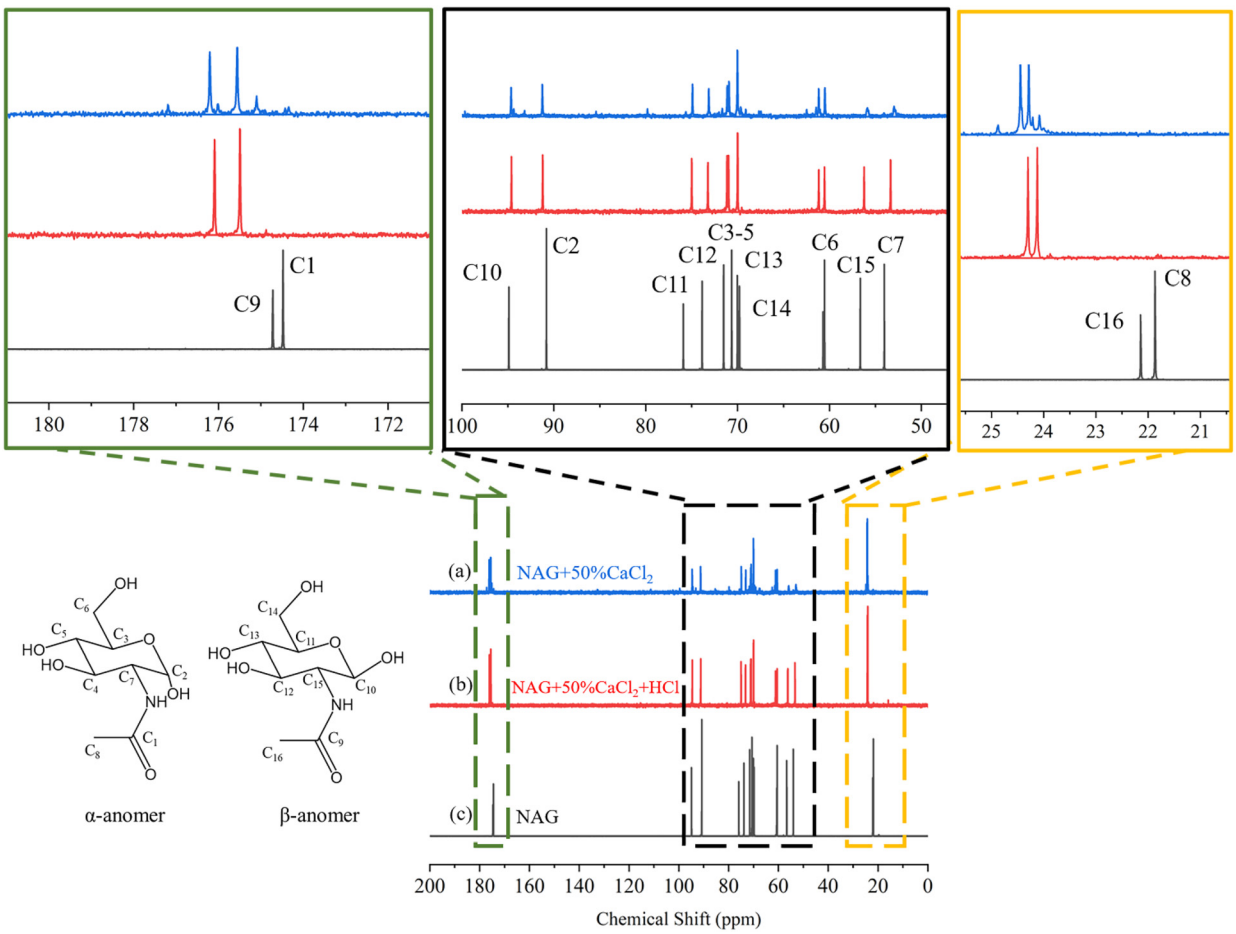

Fig. 4 ^{13}C NMR of (a) NAG, (b) NAG with HCl (30 mM HCl) and 50% $CaCl_2$ and (c) NAG with 50% $CaCl_2$. The solutions were prepared using D_2O.

acidity and the proton activity coefficient in AMSHs.[96] The $CaCl_2$ MSH-induced acidity could be responsible for chitin depolymerization without the presence of a mineral acid.

To probe the interactions of $CaCl_2$ with chitin biomass, TOF-MS, liquid- and solid-state Nuclear Magnetic Resonance (NMR) tests and X-ray photoelectron spectroscopy (XPS) were employed. A new group of Ca^{2+}-bonded oligomers were identified on TOF-MS when $CaCl_2$ was added into the soluble fractions of the aged chitin (for details, see Fig. S8†), which indicates the intensive coordination of Ca^{2+} to the chito-oligomers. Using NAG as a model compound, the ^1H and ^{13}C NMR tests were conducted in pure D_2O, 50 wt% $CaCl_2$ D_2O and acidified 50 wt% $CaCl_2$ D_2O. From the ^1H NMR spectra (see Fig. S10 and Table S6†), the signals for NAG in the unacidified or acidified $CaCl_2$ D_2O were seen to be relatively similar, but differed from that of NAG in pure D_2O. A general downfield shift (about 0.4–0.6 ppm) and peak broadening for all peaks were seen in 50 wt% $CaCl_2$ D_2O. This implies that the presence of concentrated $CaCl_2$ has altered the chemical environments of the H atoms on NAG. This agrees with the ^{13}C NMR spectra (see Fig. 4), in which general peak shifts were obviously seen in $CaCl_2$ D_2O. The detailed peak locations and assignments are listed in Table S7.† In the presence of 50 wt% $CaCl_2$, the peaks ascribed to the carbon of the C=O bond (C9 and C1) at 174.7 ppm and 174.5 ppm (β- and α-anomers) shifted to 176.2 ppm and 175.6 ppm. Meanwhile, the $-CH_3$ signals also moved from 22.2 ppm and 21.9 ppm to 24.5 ppm and 24.3 ppm. Since the oxygen atom of the C=O bond is more electronegative than that of the –OH groups, the oxophilic Ca^{2+} cation is prone to coordinate with the former one, which then leads to the downfield shifts of the carbons nearby. On the other hand, mild upfield shifts of the signals (for C10, C12, C3, *etc.*) were observed, which may be due to the Cl^- interaction with the –OH groups on the carbons. For comparison, the ^1H and ^{13}C NMR studies of NAG in concentrated $MgCl_2$ were conducted (see Fig. S11 and Tables S6 and S7†). Only very slight peak shifts were observed in $MgCl_2$ solution compared to NAG in pure water. As a result, unlike $CaCl_2$, the $MgCl_2$ solvent did not cause significant shifts of the chemical environment of NAG. Based on the above results, $CaCl_2$ exhibited extensive and strong interactions with the NAG monomer.

Solid-state ^{13}C NMR was further utilized to investigate the $CaCl_2$–chitin polymer interactions (see Fig. S12 and Table S8†). The $CaCl_2$–chitin solid sample was prepared as follows: chitin was first stirred and heated in 50 wt% $CaCl_2$ solution to promote the swelling and partial dissolution. Then the water was removed by freeze-drying. The weaker signals of the $CaCl_2$–chitin sample compared to those of the original chitin were due to the presence of a large amount of the Ca salt. The peaks that were assigned to C1 and C8 were shifted from 173.3 ppm and 23.1 ppm from those of the original chitin to 175.6 ppm and 24.2 ppm for the $CaCl_2$–chitin sample. The finding is in good agreement with the previous analyses and indicates the strong coordination of Ca^{2+} to the oxygen atom of the C=O group on the chitin polymer chains. The interactions of Cl^- with the chitin chains would cause less apparent chemical shifts compared to Ca^{2+} and might not be seen in the solid-state NMR. Aside from NMR, the chitin and $CaCl_2$–chitin samples were analyzed by XPS (see Fig. 5, Fig. S14 and Table S9†). The C 1s signals of the two samples comprise three peaks corresponding to the types of C=O (288.0 eV), C–O–C/C–OH (286.2 eV) and C–C/C–H (284.8 eV) bonds. The relative area of the middle peak considerably decreased for the $CaCl_2$–chitin sample, which might be due to the breakage of the glycosidic bonds (C–O–C) during the dissolution step. Meanwhile, the position of the C=O peak shifted slightly to 288.2 eV, indicating the interaction of the salt with chitin on this site. The O 1s spectra showed two types of peaks assigned to the C=O (532.7 eV) and C–O–C (531.2 eV) bonds, which shifted to 533.0 eV and 531.5 eV for the chitin–$CaCl_2$ sample. Such shifts were probably because the Ca^{2+} cation coordinates with the oxygen atom of the C=O group. N 1s showed a peak shift from 399.7 eV to 400.0 eV; besides, a small new peak

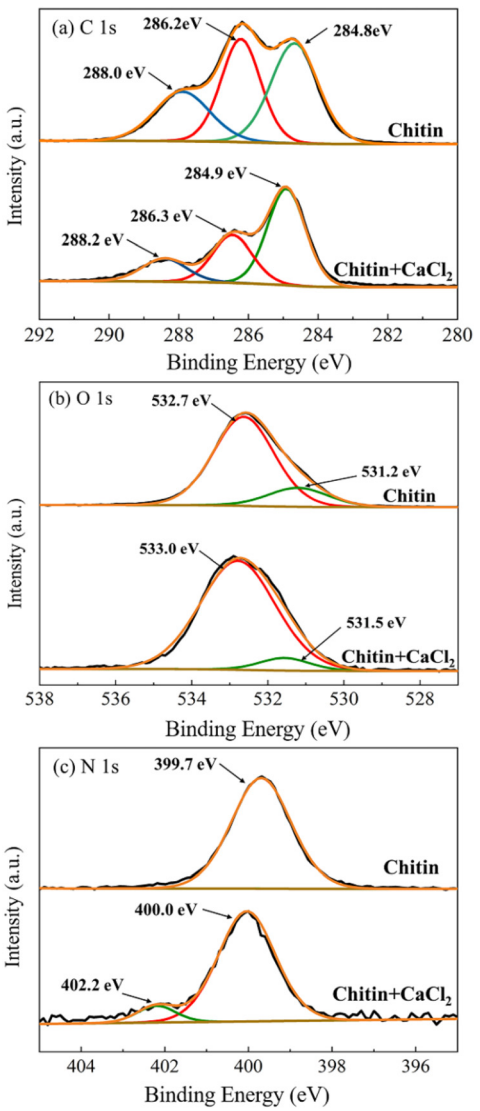

Fig. 5 (a) C 1s, (b) O 1s, and (c) N 1s XPS patterns of chitin and chitin–$CaCl_2$.

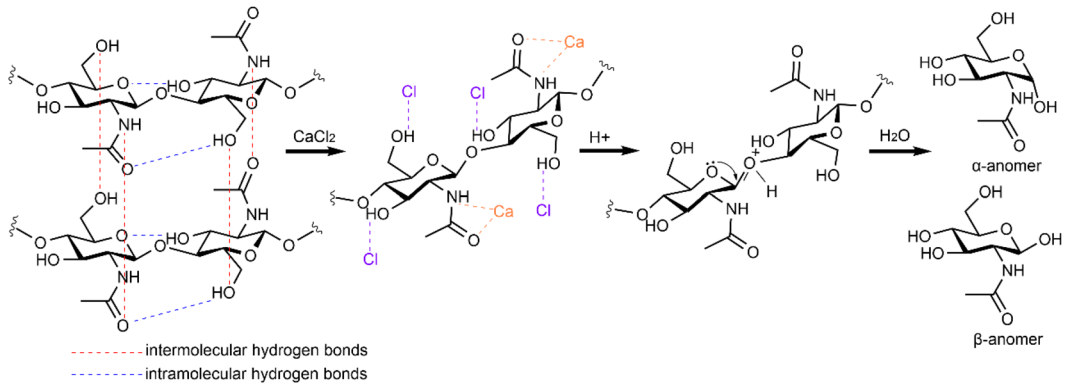

Fig. 6 Proposed interactions between the $CaCl_2$ and chitin polymer chains to promote dissolution and hydrolysis.

appeared at 402.2 eV. This possibly indicates the interaction of Ca^{2+} with the N atom on the side chain. Combining the results of various analyses, it was found that the Ca^{2+} cation would preferentially coordinate with the O atom in the C═O group and the N atom in the –NH group of chitin polymers and that Cl^- was more prone to interact with the H atoms (*e.g.* forming a hydrogen bond) of the –OH groups. Such interactions could entirely change the electronic environment of chitin and probably aid to impair the strength of the glycosidic bonds to induce facile hydrolysis (Fig. 6).

Conclusions

In this work, we put forward an integrated aging-hydrolysis approach to hydrolyze chitin into NAG in $CaCl_2$-based MSHs. The aging process is simple and mild, and $CaCl_2$ is cheap, abundant and can be waste-derived. At 393 K for a reaction time of 1 h, NAG was obtained in 51.0% and 66.8% yields from acid-aged chitin in $CaCl_2$ (50 wt%) and $CaCl_2$–$ZnBr_2$ (50 wt%–10 wt%), respectively. With aging in the presence of a small amount of H_2SO_4 (30 mM in the reaction solution), a remarkable decrease in the MW of chitin was observed. The $CaCl_2$ MSHs also showed a promotional effect on chitin depolymerization. The synergistic effect has enabled the selective production of NAG under relatively mild conditions. Based on various characterization studies, it was seen that the acid tightly bonded to chitin as active sites during aging to stimulate depolymerization, and it was seen that $CaCl_2$ and chitin interacted strongly with the Ca^{2+} cations principally bonded to the C═O/NH group on the side chain and the Cl^- anions interplayed with the –OH groups. The established protocol could add on new insights into chitin hydrolysis and contribute to the advancement of shell biorefineries.

Experimental

Materials

Chitin powder (92%, degree of acetylation (DA) was 90.7%) was purchased from Sigma-Aldrich. NAG (≥98%) was purchased from TCI Chemicals. Calcium chloride ($CaCl_2$, anhydrous, 97%), lithium chloride (LiCl, anhydrous, 98%), formic acid, and lithium bromide (LiBr, 99%) were purchased from Aladdin. Sodium chloride (NaCl, AR, 99.5%) was purchased from General Reagent. Magnesium chloride ($MgCl_2$, 99%) was purchased from Leyan. Zinc chloride ($ZnCl_2$, 98%), ferric chloride hexahydrate ($FeCl_3{\cdot}6H_2O$, 99%), potassium bromide (KBr, 99.95%), iron tribromide ($FeBr_3$, 98%) and ferrous chloride tetrahydrate ($FeCl_2{\cdot}4H_2O$, 99.95%) were purchased from Macklin. *N*,*N*-Dimethylacetamide (DMAc, 99%) was purchased from Source Leaf Organisms. 5-HMF and acetic acid were purchased from Adamas. D_2O (99.9% D, for NMR) was obtained from Energy Chemical. Hydrochloric acid (HCl, 38%), lactic acid, levulinic acid, 3A5AF and sulfuric acid (H_2SO_4, 98%) were purchased from Sinopharm Chemical Reagent. All chemicals were used without further purification.

The aging process of chitin

Aged chitin was prepared as follows: 1.66 g of chitin (8.18 mmol based on a number of NAG units) was dispersed in 5 mL of diethyl ether containing 54.3 μL of H_2SO_4 (1.02 mmol) with stirring. In the experiments to study the influence of water on the aging performance, a certain volume of water (10, 20, 60 and 80 μL) was added after the addition of H_2SO_4. The C/A ratio was initially set at 8 : 1, and other samples containing different concentrations of H_2SO_4 could be prepared as described above. At RT, diethyl ether completely evaporated after several minutes of stirring. Chitin samples containing H_2SO_4 were aged in an oven for 24–72 h, respectively, at different temperatures (RT, 313 K and 318 K). It is worth noting that all aged samples in this study are named in the format of chitin-aging temperature-aging time. For instance, chitin aged at 313 K for 48 h is denoted as chitin-313-48.

General procedures of the hydrolysis reaction

First, the various salt aqueous solutions were prepared as follows: the desired amount of salt was dissolved in deionized (DI) water to prepare a certain weight percent salt solution. As for a single type of salt, 50 wt% $CaCl_2$ was prepared by dissolving 10 g of $CaCl_2$ in 10 g of DI water. As for mixed salt

systems, 50 wt% $CaCl_2$ with 10% $ZnBr_2$ was prepared by dissolving 10 g of $CaCl_2$ in 10 g of DI water and then by dissolving 2 g of $ZnBr_2$ into the 50 wt% $CaCl_2$ solution. Different kinds of salt solutions with different concentrations were prepared in this way. Typical reactions were performed in a parallel reactor using thick-wall glass tubes sealed with PTFE caps. In each tube, 200 mg of the chitin substrate (with or without aging), 4 mL of the prepared salt solution, and a stir bar were loaded. Under reflux conditions, the reaction mixtures were heated under stirring at a specific temperature for a specific reaction time period. After the reaction, the liquid mixture was centrifuged at 8500 rpm for 5 minutes. 1 mL of the supernatant was taken and diluted to 6 mL with DI water. Due to the high concentration of the salt, the liquid was further diluted 10 times and filtered using PES (0.22 μm pore size) syringe filters before the high-performance liquid chromatography (HPLC) analysis.

Decomposition tests

The decomposition tests were conducted with pure NAG. The decomposition test is described as follows: 200 mg of pure NAG substrate and H_2SO_4 (the C/A ratio was 8 : 1) were added to 4 mL of water and 50% $CaCl_2$ solution, respectively, and stirred using a stir bar. Under condensing reflux conditions, the reaction mixtures were heated under stirring at a specific temperature for a specific time period. The NAG yield was determined as described above for the hydrolysis reaction.

Solubility tests

Solubility tests were conducted for the aged chitin samples. The solubility test procedure is described as follows: about 1 g of the aged chitin sample was weighed and added to a centrifuge tube with 30 mL of DI water, and then centrifuged at 8500 rpm for 10 minutes. The centrifugation operation was repeated 3–4 times until the pH of the solution became neutral. The remaining solids were dried overnight at 343 K in an oven. The solubility of chitin is calculated as shown below:

$$\text{Chitin solubility (wt\%)} = (\text{initial chitin (mg)} - \text{remaining solids (mg)}) \times 100\%/\text{initial chitin (mg)}.$$

NAG quantification

HPLC analysis was performed using a Shimadzu LC-20AT equipped with a spectrophotometric detector (SPD) and a refractive index detector (RID). The products were quantified using an Agilent Hi-Plex H column (7.7 × 300 mm, 8 μm) at 333 K oven temperature. 5 mM H_2SO_4 aqueous solution was used as the mobile phase with a flow rate of 0.6 mL min^{-1}. The NAG calibration curve is shown in Fig. S13.† The yield is calculated as follows (error bars indicate the standard error (n = 3)):

$$\text{Product yield (\%)} = \text{product concentration (mol L}^{-1}\text{)/initial chitin (mol product units per L)} \times 100\%.$$

Kinetic study and characterization studies

The initial rates were determined based on the slope of the NAG concentration trend at low temperatures (338–368 K) and short reaction times (20–70 min) when the NAG yield was lower than 30%. The Arrhenius plots were generated from the initial rate and $1/T$, and the slope of the Arrhenius plot was used to calculate the apparent activation energy. The viscosity average molecular weight (M_η) measurements were performed using a Ushian viscometer. A 5 wt% solution of LiCl/DMAc was prepared as a mixing solvent and different chitin samples were dissolved in LiCl/DMAc at a concentration of 0.1 wt%. The intrinsic viscosity (η) and M_η can be calculated using the following equations:

$$[\eta] = \frac{1}{c}\sqrt{2\left(\frac{t - t_0}{t_0} - \ln\frac{t}{t_0}\right)}$$

$$[\eta] = KM_\eta^\alpha$$

It should be noted that $[\eta]$ is the intrinsic viscosity. t and t_0 are the elution times of the sample and diluent. c is the concentration, and K and α are the experience constants for the polymer–solvent system at 25 °C. In this study, the constant values were c = 0.1 g dL^{-1}, K = 7.6 × 10^{-5} dL g^{-1}, and α = 0.95.[66]

Fourier transform infrared spectroscopy (FTIR) was carried out by using a Thermo Scientific Nicolet 6700 (transmission mode). The Brunauer–Emmett–Teller (BET) analysis was performed using an Autosorb-IQ3 instrument from Anton Paikanta, USA. Multifunctional X-ray diffraction (XRD) was conducted using a Bruker D8 ADVANCE Da Vinci instrument. Elemental analysis (EA) was conducted using an ELEMENT Vario EL Cube. Liquid ^{13}C Nuclear Magnetic Resonance (NMR) and ^{1}H NMR analyses were performed using a Bruker AVANCE NEO 700 MHz instrument. Solid-state ^{13}C NMR was conducted using a Bruker AVANCE NEO 600 MHz instrument. X-ray photoelectron spectroscopy (XPS) was performed using a Nexsa from Thermo Fisher Scientific. The XPS and solid-state NMR samples were lyophilized overnight before testing. It has to be noted that both XPS and solid-state ^{13}C NMR samples with $CaCl_2$ were prepared by freeze-drying: 0.5 g of chitin was mixed with 0.3 g of $CaCl_2$, and then 2–3 mL of water was added to it, heated at 313 K and stirred for 15 min, frozen overnight, and then placed into a freeze dryer for a day until it was completely dried. UHPLC/supercritical fluid chromatography-quadrupole time-of-flight mass spectrometry (TOF-MS) was performed using an Acquity 2D-UPLC/Acquity UPC2/Xevo G2-XS QTOF from Watertek; the sample is injected directly into G2-XS without UPLC and UPC2. High-resolution field emission scanning electron microscopy (SEM) was performed using a Sirion 200 from FEI, USA. Thermogravimetric analysis (TGA), derivative thermogravimetry (DTG) and differential scanning calorimetry (DSC) analysis were performed using a SDT-Q600 from TA, USA.

Conflicts of interest

There are no conflicts to declare.

Acknowledgements

This work was financially supported by the Young Scientists Fund of the National Natural Science Foundation of China (no. 21908145) and the Shenzhen Science and Technology Innovation Committee (KCXFZ20201221173413038).

References

1 W. Deng, Y. Wang, S. Zhang, K. M. Gupta, M. J. Hülsey, H. Asakura, L. Liu, Y. Han, E. M. Karp, G. T. Beckham, P. J. Dyson, J. Jiang, T. Tanaka, Y. Wang and N. Yan, *Proc. Natl. Acad. Sci. U. S. A.*, 2018, **115**, 5093–5098.
2 Y. Shao, Q. Xia, L. Dong, X. Liu, X. Han, S. F. Parker, Y. Cheng, L. L. Daemen, A. J. Ramirez-Cuesta, S. Yang and Y. Wang, *Nat. Commun.*, 2017, **8**, 16104.
3 X. Ma, G. Gözaydın, H. Yang, W. Ning, X. Han, N. Y. Poon, H. Liang, N. Yan and K. Zhou, *Proc. Natl. Acad. Sci. U. S. A.*, 2020, **117**, 7719–7728.
4 L. Li, C. Jia, X. Zhu and S. Zhang, *J. Cleaner Prod.*, 2020, **256**, 120326.
5 G. Xu, A. Wang, J. Pang, X. Zhao, J. Xu, N. Lei, J. Wang, M. Zheng, J. Yin and T. Zhang, *ChemSusChem*, 2017, **10**, 1390–1394.
6 S. S. Wong, R. Shu, J. Zhang, H. Liu and N. Yan, *Chem. Soc. Rev.*, 2020, **49**, 5510–5560.
7 L. Zhu, X. Fu, Y. Hu and C. Hu, *ChemSusChem*, 2020, **13**, 4812–4832.
8 Z. Zhang, W. Lin, Y. Li, F. Okejiri, Y. Lu, J. Liu, H. Chen, X. Lu and J. Fu, *ChemSusChem*, 2020, **13**, 4922–4928.
9 X. Chen and N. Yan, *Mater. Today Sustainability*, 2020, **7–8**, 100031.
10 C. Wang, X. Chen, M. Qi, J. Wu, G. Gözaydın, N. Yan, H. Zhong and F. Jin, *Green Chem.*, 2019, **21**, 6089–6096.
11 Y. Liu, L. Zhang, S. Feng and X. Chen, *Ind. Eng. Chem. Res.*, 2022, **61**, 10285–10293.
12 Y. Zheng, D. Xu, L. Zhang and X. Chen, *Chem. – Asian J.*, 2022, **17**, e202200556.
13 C. Zhao, S. Ju, Y. Xue, T. Ren, Y. Ji and X. Chen, *Carbon Neutrality*, 2022, **1**, 7.
14 J. Cheng and K. Cen, *Carbon Neutrality*, 2022, **1**, 11.
15 C. Xu, M. Nasrollahzadeh, M. Selva, Z. Issaabadi and R. Luque, *Chem. Soc. Rev.*, 2019, **48**, 4791–4822.
16 Y. Li, L. Shuai, H. Kim, A. H. Motagamwala, J. K. Mobley, F. Yue, Y. Tobimatsu, D. Havkin-Frenkel, F. Chen, R. A. Dixon, J. S. Luterbacher, J. A. Dumesic and J. Ralph, *Sci. Adv.*, 2018, **4**, eaau2968.
17 Z. Luo, J. Kong, B. Ma, Z. Wang, J. Huang and C. Zhao, *ACS Sustainable Chem. Eng.*, 2020, **8**, 2158–2166.
18 Y. Lu, B. Ma and C. Zhao, *ChemComm*, 2018, **54**, 9829–9832.
19 S. Song, J. Zhang, G. Gözaydın and N. Yan, *Angew. Chem., Int. Ed.*, 2019, **58**, 4934–4937.
20 Y. Wang, S. Furukawa, S. Song, Q. He, H. Asakura and N. Yan, *Angew. Chem., Int. Ed.*, 2020, **59**, 2289–2293.
21 Y. Jing, Y. Wang, S. Furukawa, J. Xia, C. Sun, M. J. Hülsey, H. Wang, Y. Guo, X. Liu and N. Yan, *Angew. Chem., Int. Ed.*, 2021, **60**, 5527–5535.
22 W. Deng, Y. Feng, J. Fu, H. Guo, Y. Guo, B. Han, Z. Jiang, L. Kong, C. Li, H. Liu, P. T. T. Nguyen, P. Ren, F. Wang, S. Wang, Y. Wang, Y. Wang, S. S. Wong, K. Yan, N. Yan, X. Yang, Y. Zhang, Z. Zhang, X. Zeng and H. Zhou, *Green Energy Environ.*, 2023, **8**(1), 10–114.
23 K. Lee, Y. Jing, Y. Wang and N. Yan, *Nat. Rev. Chem.*, 2022, **6**, 635–652.
24 Y. M. Questell-Santiago, M. V. Galkin, K. Barta and J. S. Luterbacher, *Nat. Rev. Chem.*, 2020, **4**, 311–330.
25 M. M. Abu-Omar, K. Barta, G. T. Beckham, J. S. Luterbacher, J. Ralph, R. Rinaldi, Y. Román-Leshkov, J. S. M. Samec, B. F. Sels and F. Wang, *Energy Environ. Sci.*, 2021, **14**, 262–292.
26 P. Sudarsanam, E. Peeters, E. V. Makshina, V. I. Parvulescu and B. F. Sels, *Chem. Soc. Rev.*, 2019, **48**, 2366–2421.
27 K. Tomishige, M. Yabushita, J. Cao and Y. Nakagawa, *Green Chem.*, 2022, **24**, 5652–5690.
28 D. He, X. Wang, Y. Yang, R. He, H. Zhong, Y. Wang, B. Han and F. Jin, *Proc. Natl. Acad. Sci. U. S. A.*, 2021, **118**, e2115059118.
29 X. Gao, X. Chen, J. Zhang, W. Guo, F. Jin and N. Yan, *ACS Sustainable Chem. Eng.*, 2016, **4**, 3912–3920.
30 X. Chen, S. Song, H. Li, G. Gözaydın and N. Yan, *Acc. Chem. Res.*, 2021, **54**, 1711–1722.
31 J. Wu, M. Qi, G. Gözaydın, N. Yan, Y. Gao and X. Chen, *Ind. Eng. Chem. Res.*, 2021, **60**, 3239–3248.
32 M. Qi, X. Chen, H. Zhong, J. Wu and F. Jin, *ACS Sustainable Chem. Eng.*, 2020, **8**, 18661–18670.
33 X. Chen, Y. Liu and J. Wang, *Ind. Eng. Chem. Res.*, 2020, **59**, 17008–17025.
34 X. Chen, Y. Liu and J. Wu, *Mol. Catal.*, 2020, **483**, 110716.
35 W. Deng, Q. Zhang and Y. Wang, *Catal. Today*, 2014, **234**, 31–41.
36 Y. Wang, W. Deng, B. Wang, Q. Zhang, X. Wan, Z. Tang, Y. Wang, C. Zhu, Z. Cao, G. Wang and H. Wan, *Nat. Commun.*, 2013, **4**, 2141.
37 Y. Wang, C. M. Pedersen, T. Deng, Y. Qiao and X. Hou, *Bioresour. Technol.*, 2013, **143**, 384–390.
38 Q. Meng, J. Yan, R. Wu, H. Liu, Y. Sun, N. Wu, J. Xiang, L. Zheng, J. Zhang and B. Han, *Nat. Commun.*, 2021, **12**, 4534.
39 Y. Luo, Z. Li, X. Li, X. Liu, J. Fan, J. H. Clark and C. Hu, *Catal. Today*, 2019, **319**, 14–24.
40 X. Liu, F. P. Bouxin, J. Fan, V. L. Budarin, C. Hu and J. H. Clark, *ChemSusChem*, 2020, **13**, 4296–4317.

41 T. Sagawa, H. Kobayashi, C. Murata, Y. Shichibu, K. Konishi and A. Fukuoka, *ACS Sustainable Chem. Eng.*, 2019, **7**, 14883–14888.
42 N. Yan and X. Chen, *Nature*, 2015, **524**, 155–157.
43 L. Yuan, Y. Hu, X. Guo, G. Li, A. Wang, Y. Cong, F. Wang, T. Zhang and N. Li, *Chem Catal.*, 2022, **2**, 2302–2311.
44 Y. Liu, C. Li, W. Miao, W. Tang, D. Xue, C. Li, B. Zhang, J. Xiao, A. Wang, T. Zhang and C. Wang, *ACS Catal.*, 2019, **9**, 4441–4447.
45 H. Su, J. Wang and L. Yan, *ACS Sustainable Chem. Eng.*, 2019, **7**, 18476–18482.
46 S. Jiang, H. Jiang, Y. Zhou, S. Jiang and G. Zhang, *Bioprocess Biosyst. Eng.*, 2019, **42**, 611–619.
47 H. Chen, J. Wang, Y. Yao, Z. Zhang, Z. Yang, J. Li, K. Chen, X. Lu, P. Ouyang and J. Fu, *ChemElectroChem*, 2019, **6**, 5797–5801.
48 S. Dutta, I. K. M. Yu, D. C. W. Tsang, Z. Su, C. Hu, K. C. W. Wu, A. C. K. Yip, Y. S. Ok and C. S. Poon, *Bioresour. Technol.*, 2020, **298**, 122544.
49 Y. Ohmi, S. Nishimura and K. Ebitani, *ChemSusChem*, 2013, **6**, 2259–2262.
50 M. Osada, K. Kikuta, K. Yoshida, K. Totani, M. Ogata and T. Usui, *Green Chem.*, 2013, **15**, 2960–2966.
51 T.-W. Tzeng, P. Bhaumik and P.-W. Chung, *Mol. Catal.*, 2019, **479**, 110627.
52 H. Zang, J. Lou, S. Jiao, H. Li, Y. Du and J. Wang, *J. Mol. Liq.*, 2021, **330**, 115667.
53 J. Wang, H. Zang, S. Jiao, K. Wang, Z. Shang, H. Li and J. Lou, *Sci. Total Environ.*, 2020, **710**, 136293.
54 Y. Liu and F. M. Kerton, *Pure Appl. Chem.*, 2021, **93**, 463–478.
55 Z. Cai, R. Chen, H. Zhang, F. Li, J. Long, L. Jiang and X. Li, *Green Chem.*, 2021, **23**, 10116–10122.
56 H. Li, H. Guo, Z. Fang, T. M. Aida and R. L. Smith, *Green Chem.*, 2020, **22**, 582–611.
57 D. Rodríguez-Padrón, D. Zhao, C. Carrillo-Carrion, C. Morales-Torres, A. M. Elsharif, A. M. Balu, R. Luque and C. Len, *Catal. Today*, 2021, **368**, 243–249.
58 X. Chen, H. Yang and N. Yan, *Chem. – Eur. J.*, 2016, **22**, 13402–13421.
59 M. Mascal and E. B. Nikitin, *ChemSusChem*, 2009, **2**, 859–861.
60 M. W. Drover, K. W. Omari, J. N. Murphy and F. M. Kerton, *RSC Adv.*, 2012, **2**, 4642–4644.
61 X. Chen, S. L. Chew, F. M. Kerton and N. Yan, *Green Chem.*, 2014, **16**, 2204–2212.
62 M. J. Hülsey, B. Zhang, Z. Ma, H. Asakura, D. A. Do, W. Chen, T. Tanaka, P. Zhang, Z. Wu and N. Yan, *Nat. Commun.*, 2019, **10**, 1330.
63 M. J. Hülsey, V. Fung, X. Hou, J. Wu and N. Yan, *Angew. Chem., Int. Ed.*, 2022, **61**, e202208237.
64 L. Lin, X. Han, B. Han and S. Yang, *Chem. Soc. Rev.*, 2021, **50**, 11270–11292.
65 B. Duan, Y. Huang, A. Lu and L. Zhang, *Prog. Polym. Sci.*, 2018, **82**, 1–33.
66 H. Yang, G. Gözaydın, R. R. Nasaruddin, J. R. G. Har, X. Chen, X. Wang and N. Yan, *ACS Sustainable Chem. Eng.*, 2019, **7**, 5532–5542.
67 A. Zhang, G. Wei, X. Mo, N. Zhou, K. Chen and P. Ouyang, *Green Chem.*, 2018, **20**, 2320–2327.
68 A. Zhang, C. Gao, J. Wang, K. Chen and P. Ouyang, *Green Chem.*, 2016, **18**, 2147–2154.
69 A. Ajavakom, S. Supsvetson, A. Somboot and M. Sukwattanasinitt, *Carbohydr. Polym.*, 2012, **90**, 73–77.
70 M. Yabushita, H. Kobayashi, K. Kuroki, S. Ito and A. Fukuoka, *ChemSusChem*, 2015, **8**, 3760–3763.
71 G. Margoutidis, V. H. Parsons, C. S. Bottaro, N. Yan and F. M. Kerton, *ACS Sustainable Chem. Eng.*, 2018, **6**, 1662–1669.
72 J. Zhang and N. Yan, *Green Chem.*, 2016, **18**, 5050–5058.
73 Y. Pierson, X. Chen, F. D. Bobbink, J. Zhang and N. Yan, *ACS Sustainable Chem. Eng.*, 2014, **2**, 2081–2089.
74 J. Zhang and N. Yan, *ChemCatChem*, 2017, **9**, 2790–2796.
75 N. Rodriguez Quiroz, A. M. Norton, H. Nguyen, E. Vasileiadou and D. G. Vlachos, *ACS Catal.*, 2019, **9**, 9923–9952.
76 N. Li, X. Pan and J. Alexander, *Green Chem.*, 2016, **18**, 5367–5376.
77 W. Deng, J. R. Kennedy, G. Tsilomelekis, W. Zheng and V. Nikolakis, *Ind. Eng. Chem. Res.*, 2015, **54**, 5226–5236.
78 S. Sadula, O. Oesterling, A. Nardone, B. Dinkelacker and B. Saha, *Green Chem.*, 2017, **19**, 3888–3898.
79 J. van den Bergh, I. V. Babich, P. O'Connor and J. A. Moulijn, *Ind. Eng. Chem. Res.*, 2017, **56**, 13423–13433.
80 P. L. Ragg, P. R. Fields, P. B. Tinker, B. S. Hartley, P. M. A. Broda and P. J. Senior, *Philos. Trans. R. Soc., A*, 1987, **321**, 537–547.
81 S. Fischer, K. Thümmler, K. Pfeiffer, T. Liebert and T. Heinze, *Cellulose*, 2002, **9**, 293–300.
82 H. Zhang, N. Li, X. Pan, S. Wu and J. Xie, *ACS Sustainable Chem. Eng.*, 2017, **5**, 4066–4072.
83 G. Gözaydın, S. Song and N. Yan, *Green Chem.*, 2020, **22**, 5096–5104.
84 M. Chen, Q. Liu, S.-W. Wang, E. Wang, X. Guo and S.-L. Chou, *Adv. Energy Mater.*, 2019, **9**, 1803609.
85 C. Xu, B. Li, H. Du and F. Kang, *Angew. Chem., Int. Ed.*, 2012, **51**, 933–935.
86 K. M. Abraham, *ACS Energy Lett.*, 2020, **5**, 3544–3547.
87 C. Sasaki, T. Nakagawa, C. Asada and Y. Nakamura, *Waste Biomass Valorization*, 2020, **11**, 4279–4287.
88 M. Linde, E.-L. Jakobsson, M. Galbe and G. Zacchi, *Biomass Bioenergy*, 2008, **32**, 326–332.
89 K. H. Kim, M. Tucker and Q. Nguyen, *Bioresour. Technol.*, 2005, **96**, 1249–1255.
90 C. Tengborg, K. Stenberg, M. Galbe, G. Zacchi, S. Larsson, E. Palmqvist and B. Hahn-Hägerdal, *Appl. Biochem. Biotechnol.*, 1998, **70**, 3.
91 F. Shen, X. Xiong, J. Fu, J. Yang, M. Qiu, X. Qi and D. C. W. Tsang, *Renewable Sustainable Energy Rev.*, 2020, **130**, 109944.

92 F. Hajiali, T. Jin, G. Yang, M. Santos, E. Lam and A. Moores, *ChemSusChem*, 2022, **15**, e202102535.
93 H. Kobayashi, Y. Suzuki, T. Sagawa, K. Kuroki, J.-y. Hasegawa and A. Fukuoka, *Phys. Chem. Chem. Phys.*, 2021, **23**, 15908–15916.
94 H.-H. Emons, *Electrochim. Acta*, 1988, **33**, 1243–1250.
95 Q. Liu, Q. Ma, S. Sabnis, W. Zheng, D. G. Vlachos, W. Fan, W. Li and L. Ma, *Green Chem.*, 2019, **21**, 5030–5038.
96 N. Rodriguez Quiroz, A. M. D. Padmanathan, S. H. Mushrif and D. G. Vlachos, *ACS Catal.*, 2019, **9**, 10551–10561.
97 T. Friščić, S. L. Childs, S. A. A. Rizvi and W. Jones, *CrystEngComm*, 2009, **11**, 418–426.
98 T. Di Nardo, C. Hadad, A. Nguyen Van Nhien and A. Moores, *Green Chem.*, 2019, **21**, 3276–3285.
99 J.-L. Do and T. Friščić, *ACS Cent. Sci.*, 2017, **3**, 13–19.
100 G. Liu, Y. Xie, C. Wei, C. Liu, F. Song, X. Sun, Y. Zhang and H. Cui, *Biomass Bioenergy*, 2022, **158**, 106363.
101 A. Gautam and T. J. Menkhaus, *J. Membr. Sci.*, 2014, **451**, 252–265.
102 Q. Liu, S. Luo, W. Fan, X. Ouyang and X. Qiu, *Green Chem.*, 2021, **23**, 4114–4124.
103 X. Chen, Y. Gao, L. Wang, H. Chen and N. Yan, *ChemPlusChem*, 2015, **80**, 1565–1572.